

# Multiple-Transmitter Achieving Load-Independent Transmitter Current and Compensation of Cross-Interference Among Transmitters for Wide Charging Area Wireless Power Transfer Systems

Kodai Matsuura, Masataka Ishihara, Akihiro Konishi Kazuhiro, Umetani, Eiji Hiraki  
Graduate School of Natural Science and Technology  
Okayama University  
Okayama, Japan

Published in: 2020 IEEE Energy Conversion Congress and Exposition (ECCE)

© 2020 IEEE. Personal use of this material is permitted. Permission from IEEE must be obtained for all other uses, in any current or future media, including reprinting/republishing this material for advertising or promotional purposes, creating new collective works, for resale or redistribution to servers or lists, or reuse of any copyrighted component of this work in other works.

DOI: 10.1109/ECCE44975.2020.9235430

# Multiple-Transmitter Achieving Load-Independent Transmitter Current and Compensation of Cross-Interference Among Transmitters for Wide Charging Area Wireless Power Transfer Systems

Kodai Matsuura  
Graduate School of Natural  
Science and Technology  
Okayama University  
Okayama, Japan  
pd1p0ifd@s.okayama-u.ac.jp

Masataka Ishihara  
Graduate School of Natural  
Science and Technology  
Okayama University  
Okayama, Japan  
p4wv0vf6@s.okayama-u.ac.jp

Akihiro Konishi  
Graduate School of Natural  
Science and Technology  
Okayama University  
Okayama, Japan  
p3448o58@s.okayama-u.ac.jp

Kazuhiro Umetani  
Graduate School of Engineering  
Tohoku University  
Sendai, Japan  
kazuhiro.umetani.e1@tohoku.ac.jp

Eiji Hiraki  
Graduate School of Natural  
Science and Technology  
Okayama University  
Okayama, Japan  
hiraki@okayama-u.ac.jp

**Abstract**—Recently, a resonant inductive coupling wireless power transfer (RIC-WPT) system with multiple transmitters is emerging as a promising power supply method for household appliances, mobile devices, and wearable devices dispersedly placed in a wide area. However, the multiple-transmitter often suffers from an unstable operation of an inverter, feeding AC current to the transmitter coil, due to the cross-interference (i.e., cross-coupling) among the transmitters. When the cross-interference occurs, the inverter may not achieve high power factor and soft switching, which damages the power density and reliability of the multiple-transmitter. Therefore, this paper proposes a multiple-transmitter, including its controller, that can compensate for the effect of the cross-interference. In the proposed multiple-transmitter, each transmitter has a simple switching circuit that can automatically cancel the induced voltage due to the cross-interference with only simple control. Furthermore, the proposed multiple-transmitter also achieves a load-independent transmitter current by the control of the input voltage of the inverter, which results in a stable magnetic field regardless of load variation. Experiments verify the effectiveness and appropriateness of the proposed multiple-transmitter.

**Keywords**—wireless power transfer, resonant inductive coupling, multiple transmitters, cross-coupling, automatic active compensation, load-independent transmitter current

## I. INTRODUCTION

Recently, resonant inductive coupling wireless power transfer (RIC-WPT) systems with multiple-transmitter are widely studied for various applications. One attractive application of the RIC-WPT system is a wireless charging desk [1, 2] shown in Fig. 1 that can supply electric power to multiple household appliances, mobile devices, and wearable devices placed at the free position of the desk. The wireless charging desk can improve not only user convenience but also safety due to the elimination of electrical outlets and tangled cables.

Fig. 2 shows the typical multiple-transmitter RIC-WPT system, where  $W_{TXi}$  ( $i=1, \dots, n$ ) are the transmitter coils, and  $W_{RX}$  is the receiver coil. The inverter in the transmitter feeds

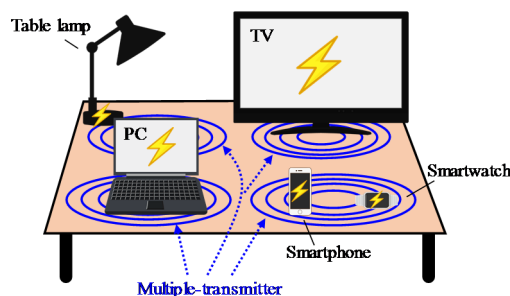


Fig. 1. Wireless charging desk.

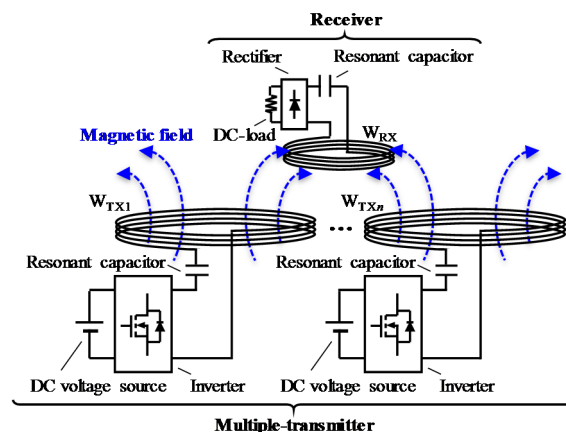


Fig. 2. Typical multiple-transmitter RIC-WPT system.

an AC current to the transmitter resonator composed of the transmitter coil and the resonant capacitor, which results in an AC magnetic field. The receiver rectifies the receiver current excited by the AC magnetic field and obtains the DC power. Usually, to achieve zero voltage switching (ZVS) turn-on and high power factor of the inverter simultaneously, the resonant frequency of the transmitter resonator is designed so that the transmitter resonator is slightly inductive at the operating frequency. Furthermore, in the application such as the wireless charging desk where a single transmitter may charge multiple-receiver, a constant transmitter current independent of a load variation is usually required [3–6]. If the load-independent

transmitter current can be achieved, the output power of each receiver is not affected by other receivers in the cases where the magnetic coupling among receivers can be neglected [5, 6]. The load-independent transmitter current can be obtained by the feedback control of the DC voltage source or inverter [7] or the LCC inverter [8–10].

As pointed in [9, 11], for a wide charging area RIC-WPT system, the WPT using the multiple-transmitter is superior to the WPT using a single large transmitter because the coupling coefficients between the transmitters and receivers as well as the quality factors of the transmitters can be increased. One of the attractive usage forms of the multiple-transmitter is controlling the effective value of the transmitter current according to the position of the receiver while maintaining the load-independent transmitter current. For example, transmitters having weak coupling with a receiver are turned off, and only transmitters having strong coupling with the receiver are turned on. As a result, a useless AC magnetic field in the place without the receiver is suppressed, and the efficiency can be improved owing to the reduction of the copper loss [9, 11]. Furthermore, as discussed in [11], the efficiency further can be improved by controlling the ratio of each transmitter current according to the ratio of the mutual inductance between each transmitter coil and the receiver coil.

Despite the attractive advantages, the multiple-transmitter often suffers from the unstable operation of the inverter due to the cross-interference among transmitters [9, 10, 12]. This cross-interference also have been referred to as cross-coupling in several previous studies [9–12]. The cross-interference is caused by an induced voltage due to the magnetic coupling among transmitter coils. This induced voltage changes the amplitude and phase of the current in the inverter. As a result, when the cross-interference occurs, the power factor of the inverter probably decreases. Consequently, the DC voltage source and inverter require a high VA rating to obtain the same current as in the absence of the cross-interference. In the worst case, if the transmitter resonator equivalently becomes capacitive due to the cross-interference, the switching loss of the inverter may significantly increase because of hard switching.

To solve this problem, many conventional studies compensated for the cross-interference effect by inserting an appropriate fixed capacitance to each transmitter resonator manually [5, 6]. The voltage generated in the appropriate capacitance can fully cancel the induced voltage due to the cross-interference, resulting in the compensation of the cross-interference. However, this approach suffers from the difficulty that an appropriate capacitance depends on other transmitter currents and mutual inductances among transmitter coils. Therefore, a fixed capacitance cannot compensate for the cross-interference effect of a RIC-WPT system where each transmitter current changes according to the position of a receiver. Certainly, if all transmitters are driven always with a constant transmitter current at a fixed position, an appropriate capacitance for each transmitter is determined uniquely. However, even in this condition, it is practically difficult to fully eliminate the cross-interference effect because the capacitance often deviates from a designed value due to manufacturing tolerances or the aging effect. Hence, an inserted capacitance must be controlled dynamically.

Therefore, this paper proposes a multiple-transmitter that can achieve the full compensation of the cross-interference

among transmitters and the load-independent current dynamically. First, the load-independent current is realized by using the DC-DC converter with the feedback control. The DC-DC converter controls the input voltage of the inverter so that the amplitude of the transmitter current is constant. Then, the compensation of the cross-interference regardless of the adjacent transmitter operations is achieved by dynamically controlling the variable reactance inserted into each transmitter. Conventionally, the control of the variable reactance has been thought to be difficult because the real-time estimation of many circuit parameters (e.g., other transmitter currents and mutual inductances among transmitters) is needed. However, in this paper, we reveal a control concept for the variable reactance that does not require the estimation of circuit parameters relating to other transmitters. The control concept only uses the phase difference between the transmitter current and the output voltage of the inverter in the corresponding transmitter. In order to realize the control strategy, we applied a simple switching circuit named automatic tuning assist circuit (ATAC). The ATAC was originally proposed in [13] to solve the problem that the resonant frequency of the transmitter deviates from the designed value due to manufacturing tolerances or the aging effect of the transmitter resonator. However, this paper utilizes the ATAC to compensate for the cross-interference among the transmitters. Due to the advantage of the ATAC, the proposed multiple-transmitter RIC-WPT system can achieve the control concept revealed in this paper without even sensing the phase difference between the transmitter current and the output voltage of the inverter. The basic idea of the proposed multiple-transmitter is the technique to compensate for the cross-interference of multiple receivers proposed in [6]. In [6], for eliminating the effect of cross-interference among receiver coils, the ATAC is inserted to each receiver. In this paper, we also propose a controller for the ATAC and a controller for achieving the load-independent transmitter current, which is not discussed in [6].

The remainder of this paper is structured into four sections. Section II shows the proposed multiple-transmitter for eliminating the cross-interference effect. Section III discusses a practical implementation of the proposed multiple-transmitter including its controller. Section IV presents experiments to verify the effectiveness and appropriateness of the proposed multiple-transmitter. Finally, section V gives the conclusions.

## II. RIC-WPT SYSTEM WITH PROPOSED MULTIPLE-TRANSMITTER

In this section, we first explain the concept for controlling the variable reactance without sensing the other transmitter current and the mutual inductance among the transmitters. Next, we explain the system configuration of the proposed multiple-transmitter based on the concept and the operating principle.

In the rest of this paper, we discuss the RIC-WPT system with two transmitters for simplifying analysis. However, the analysis result in this section can be extended for the RIC-WPT system with more than two transmitters. Furthermore, we assume that the quality factor of each transmitter is high enough for the first harmonic approximation analysis.

### A. Concept for Controlling Variable Reactance

Fig. 3 shows the concept diagram of the proposed multiple-transmitter RIC-WPT system. As depicted in Fig. 3,

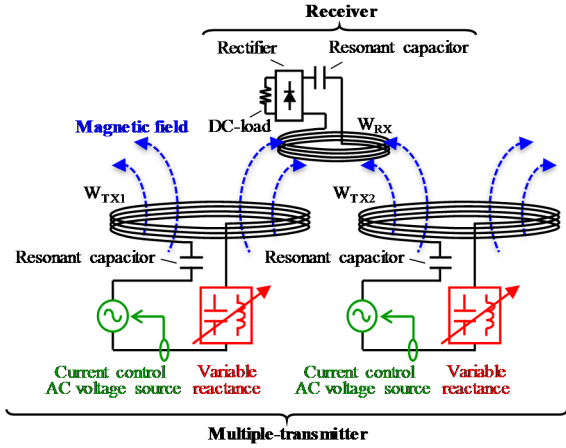


Fig. 3. Concept diagram of proposed multiple-transmitter RIC-WPT system.

each transmitter has the current control AC voltage source instead of a constant amplitude AC voltage source, and the variable reactance is connected in series to the transmitter resonator. The current control AC voltage source generates AC voltage so that the amplitude of the transmitter current is constant regardless of a load variation. The variable reactance is implemented to compensate for the cross-interference effect.

Fig. 4 shows the equivalent circuit of Fig. 3. In this figure,  $V_{inv1}$  and  $V_{inv2}$  are the fundamental output voltages of the inverters, respectively;  $\omega$  is the operating angular frequency;  $I_1$ ,  $I_2$ , and  $I_r$  are the currents in transmitters and a receiver, respectively;  $C_1$ ,  $C_2$ , and  $C_r$  are the capacitances of the resonant capacitors, respectively;  $L_1$ ,  $L_2$ , and  $L_r$  are the self-inductances of  $W_{TX1}$ ,  $W_{TX2}$ , and  $W_{RX}$ , respectively;  $r_1$ ,  $r_2$ , and  $r_r$  are the parasitic resistances of  $W_{TX1}$ ,  $W_{TX2}$ , and  $W_{RX}$ , respectively;  $X_{adj1}$  and  $X_{adj2}$  are the inserted variable reactance to each transmitter, respectively;  $R$  is equivalent of the AC load;  $M_{1r}$  and  $M_{2r}$  are the mutual inductances between each transmitter coil and the receiver coil, respectively;  $M_{12}$  is the mutual inductance among transmitter coils, which causes the cross-interference among the transmitters.

In this study, in order to compensate for the cross-interference effect, we control the variable reactance based on the phase difference between the output voltage of the inverter and the transmitter current. Specifically, we control the variable reactance so that the phase difference between the transmitter current and the output voltage of the inverter is constant from the predetermined phase, regardless of the operation of the other transmitter. The phase difference is designed so that ZVS turn-on and high power factor of the inverter can be achieved. In the proposed multiple-transmitter RIC-WPT system, the designed phase difference must be the same for all transmitters. Furthermore, the phase angles of  $V_{inv1}$  and  $V_{inv2}$  must be identical. Fig. 5 shows the phasor diagrams of each transmitter in this condition, where  $X_1 = \omega L_1 - 1/\omega C_1$  and  $X_2 = \omega L_2 - 1/\omega C_2$ ;  $I_1$ ,  $I_2$ ,  $V_{inv1}$ , and  $V_{inv2}$  are the effective values of  $I_1$ ,  $I_2$ ,  $V_{inv1}$ , and  $V_{inv2}$ , respectively;  $\alpha$  is the designed phase difference between  $V_{inv1}$  (or  $V_{inv2}$ ) and  $I_1$  (or  $I_2$ ). As shown in Fig. 5, the induced voltage due to the magnetic coupling between transmitters is orthogonal to the current in each transmitter because of each transmitter current in phase. Applying Kirchhoff's voltage law to Fig. 5, the relationship in the phasors, which are orthogonal to the transmitter current, can be derived as

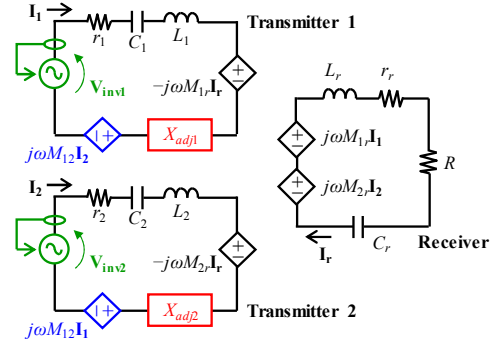


Fig. 4. Equivalent circuit of Fig. 3.

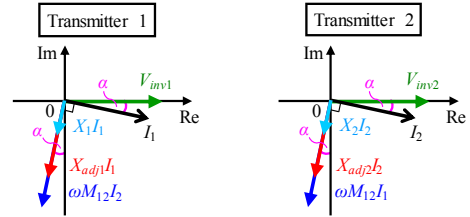


Fig. 5. Phasor diagrams of each transmitter in Fig. 4.

$$X_{adj1}I_1 = -X_1I_1 - \omega M_{12}I_2 + V_{inv1} \sin \alpha \quad (1)$$

$$X_{adj2}I_2 = -X_2I_2 - \omega M_{12}I_1 + V_{inv2} \sin \alpha \quad (2)$$

According to (1) and (2), the induced voltage due to the magnetic coupling between the transmitters behaves as a pure reactance in each transmitter and, thus, inserting variable reactance can eliminate the induced voltage completely. Therefore, each transmitter can compensate for the effect of the cross-interference fully without sensing the current in other transmitters and the mutual inductance among the transmitters. Furthermore, (1) and (2) indicate that the variable reactances can cancel the voltage drops of  $X_1$  and  $X_2$ . This result means that the control concept revealed in this paper also can eliminate the effect due to the deviation of the resonant frequency from the designed value.

### B. Overview of Proposed Multiple-Transmitter RIC-WPT System

Then, this subsection describes the specific configurations of the current control AC voltage source and the variable reactance of Fig. 3. Fig. 6 shows the system configuration of the proposed multiple-transmitter RIC-WPT system.

First, the current control AC voltage source is realized by the DC-DC converter and the inverter as shown in Fig. 6, where  $V_{i1}$  and  $V_{i2}$  are the input DC voltages for the DC-DC converters;  $V_{i\_inv1}$ ,  $V_{i\_inv2}$  are the input DC voltages for the inverters. The controller of the DC-DC converters senses the amplitude of the transmitter current and generates control signals for the DC-DC converter. As a result, the DC-DC converters control  $V_{i\_inv1}$  and  $V_{i\_inv2}$  so that the amplitude of each transmitter current is constant.

Next, we applied the ATAC to each transmitter as the variable reactance as shown in Fig. 6. Certainly, several techniques have been recently proposed to configure a variable reactance other than the ATAC such as a capacitor matrix [15–17], DC-voltage-controlled variable capacitor [18], gate-controlled series capacitor [19], mechanical variable capacitor controlled by the stepping motor [20], and variable inductor [21, 22]. However, to achieve the control concept revealed in this paper, the ATAC may be appropriate because

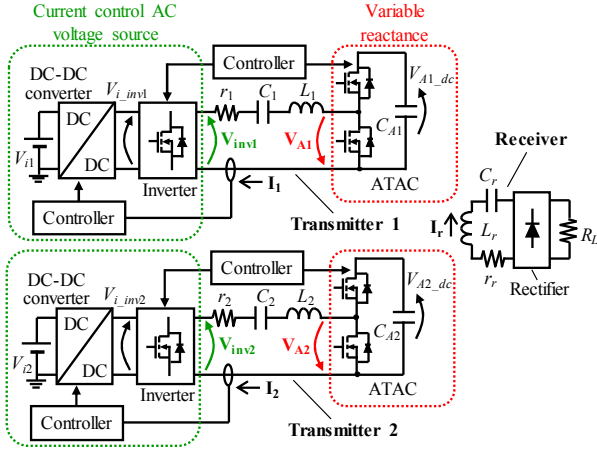


Fig. 6. System configuration of proposed multiple-transmitter RIC-WPT system.

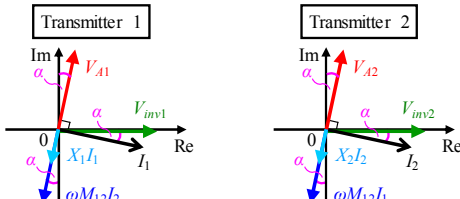


Fig. 7. Phasor diagrams of each transmitter in Fig. 6.

it can control the phase difference between the output voltage of the inverter and the transmitter current without sensing those, as explained in the next subsection.

### C. Operating Principle of ATAC for Compensation of Cross-Interference Effect

The ATAC consists of the half-bridge circuit and the smoothing capacitor only, which is connected to each transmitter resonator in series, as depicted in Fig. 6.  $C_{A1}$  and  $C_{A2}$  are the smoothing capacitor of the ATAC, respectively;  $V_{A1}$  and  $V_{A2}$  are the fundamental output voltages of the ATAC, respectively;  $V_{A1\_dc}$  and  $V_{A2\_dc}$  are the DC voltages appearing at the smoothing capacitors of the ATAC, respectively. The capacitance of the smoothing capacitor is designed to be large enough for the resonant capacitor. Hence, the smoothing capacitor has little influence on the resonant frequency. A DC voltage is generated in the smoothing capacitor. However, any DC voltage supply is not needed at the DC bus of the half-bridge circuit because the ATAC automatically generates the DC voltage by the transmitter current. The half-bridge circuit of the ATAC operates at the same frequency as the switching frequency of the inverter, but at the constant phase-shifted from the inverter. In addition to this, the duty ratio of the half-bridge circuit of the ATAC is designed to be 50%. Hence, the ATAC behaves to apply a rectangular voltage to the transmitter resonator.

The ATAC has no resistive components ideally because the ATAC consists of the half-bridge circuit and the smoothing capacitor only. Therefore, the ATAC should not receive effective power in the steady-state. In other words, the phase difference between the transmitter current and the output voltage of the ATAC must be  $\pi/2$  in the steady-state. Hence, if the phase of the output voltage of the ATAC is designed in advance, the phase of the transmitter current is automatically determined so that its phase is orthogonal to that of the output voltage of the ATAC. Therefore, the ATAC behaves as the variable reactance which can fix the phase of

the transmitter current against that of the output voltage of the ATAC without sensing the phase of the current in its transmitter.

In order to achieve the control concept, the phase of the output voltage of the ATAC is fixed to be  $\pi/2 - \alpha$  against that of the output voltage of the inverter in each transmitter. In this condition, the phasor diagrams of Fig. 6 must be Fig. 7 in the steady-state. In Fig. 7,  $V_{A1}$  and  $V_{A2}$  are the effective value of the  $V_{A1}$  and  $V_{A2}$ , respectively. As depicted in Fig. 7, the induced voltage due to the magnetic coupling between transmitters is orthogonal to the transmitter current because of each transmitter current in phase. Applying Kirchoff's voltage law to Fig. 7, the relationship in the phasors, which are orthogonal to the transmitter current, can be derived as

$$V_{A1} = X_1 I_1 + \omega M_{12} I_2 - V_{inv1} \sin \alpha \quad (3)$$

$$V_{A2} = X_2 I_2 + \omega M_{12} I_1 - V_{inv2} \sin \alpha \quad (4)$$

According to (3) and (4), the induced voltage due to the magnetic coupling among transmitters behaves as a pure reactance and, thus, the output voltage of the ATAC can eliminate the induced voltage completely. Furthermore, the output voltage of the ATAC is automatically generated in order to keep  $\alpha$  even if the cross-interference occurs. Therefore, applying the ATAC, the control concept can be realized without sensing the phase of the current and the output voltage of the inverter in the corresponding transmitter.

In order to suppress the power loss in the operation of the ATAC, the ATAC must achieve ZVS turn-on. As depicted in Fig. 7, each transmitter current lags behind the output voltage of the ATAC. In this condition, the ATAC can operate at ZVS turn-on. However, if the output voltage of the ATAC is negative, each transmitter current leads against the output voltage of the ATAC. Consequently, the switching operation of the ATAC becomes hard switching and, accordingly, the power loss of the ATAC may significantly increase. According to (3) and (4), whether the output voltage is positive or negative depends on the polarity of the mutual inductance, the reactance, and the output voltage of the inverter. Therefore, in order to avoid hard switching of the half-bridge circuit of the ATAC, under expected circuit parameters, each reactance of the transmitter resonator should be determined to be the output voltage of the ATAC is positive in advance.

### III. PRACTICAL IMPLEMENTATION OF PROPOSED MULTIPLE-TRANSMITTER

Fig. 8 shows the practical circuit configuration of each transmitter of Fig. 6. As shown in Fig. 8, this paper adopts the synchronous buck converter as the DC-DC converter.

The proposed transmitter has two independent controllers. Note that the signal generator as depicted in Fig. 8 is common in each transmitter. First, the block diagram surrounded by the dotted red lines indicates the schematic of the controller of the synchronous buck converter to achieve load-independent current. Then, the block diagram surrounded by the dotted blue lines indicates the schematic of the controller of the inverter and the ATAC. As shown in Fig. 8, the controller of the ATAC only consists of the phase shift circuit and gate driver because the ATAC only needs to operate with a fixed phase difference from the output voltage of the inverter, as discussed in Section II-C.

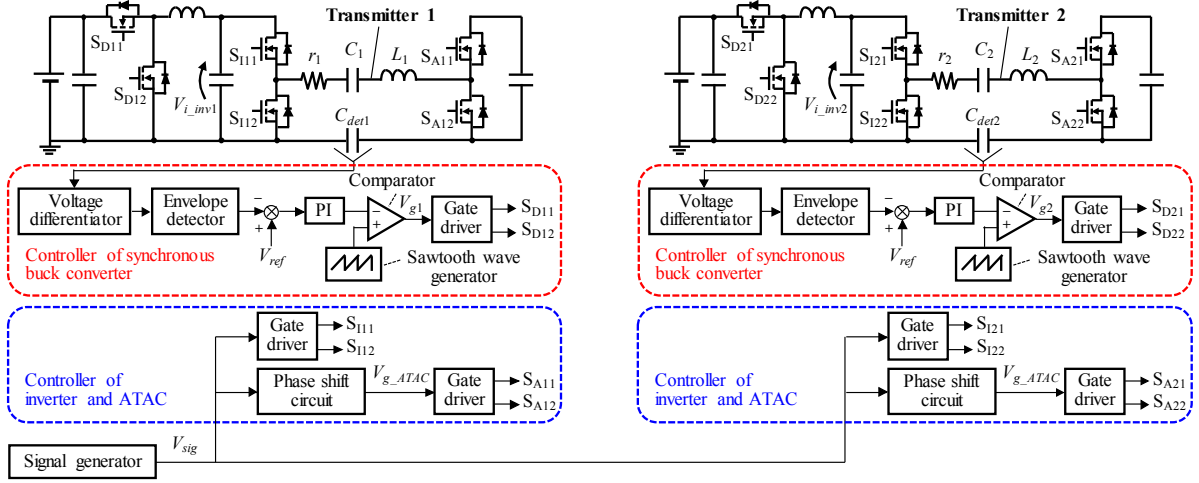


Fig. 8. Practical circuit configuration including controllers of each transmitter.

The circuit configurations of the controllers are the same in each transmitter. Hence, in the following subsection, we describe the detailed circuit configurations of the controllers in transmitter 1.

### A. Controller of Synchronous Buck Converter

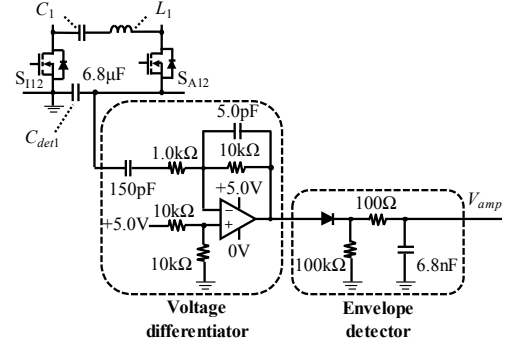
Fig. 9 shows the detailed circuit configurations of the controller for the synchronous buck converter in transmitter 1. The controller adjusts the duty ratio of the  $S_{D11}$  and  $S_{D12}$  to achieve the load-independent transmitter current.

Fig. 9 (a) shows the sensing circuit of the amplitude of the transmitter current. This circuit is comprised of the voltage differentiator and the envelope detector. The voltage differentiator detects the transmitter current by differentiating the voltage appearing at  $C_{det1}$ , which is the additional capacitor inserted to the transmitter resonator.  $C_{det1}$  is designed to be a larger value than  $C_1$  not to exceed the voltage rating of the differentiator. Then, the voltage appearing at  $C_{det1}$  is converted to the DC voltage  $V_{amp}$ , the amplitude of the output voltage of the differentiator, by the envelope detector.  $V_{amp}$  is proportional to the transmitter current amplitude and, thus, the circuit detects the current amplitude indirectly.

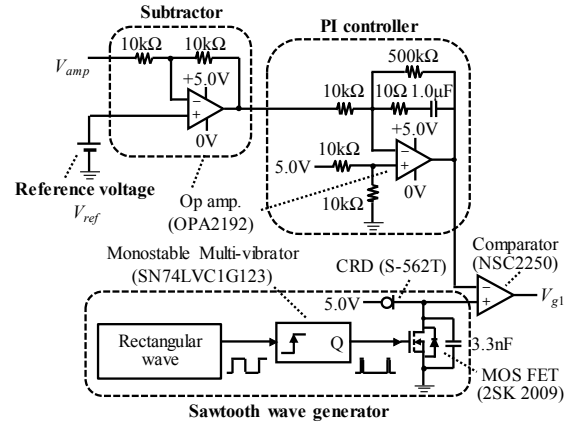
Fig. 9 (b) shows the circuit of generating the gating signal for the synchronous buck converter. This circuit is comprised of the subtractor, the PI controller, the sawtooth wave generator, and the comparator. The reference voltage  $V_{ref}$  is determined according to the desired value of the transmitter current amplitude. The error between  $V_{amp}$  and  $V_{ref}$  by the subtractor is input to the PI controller. Then, the output voltage of the PI controller is compared with the sawtooth wave to generate the signal  $V_{g1}$  for the gate driver of the synchronous buck converter.

### B. Controller of ATAC

Fig. 10 shows the circuit configuration of the phase shift circuit and its key waveforms. As shown in Fig. 10 (a),  $V_{sig}$  is converted to the double frequency sawtooth wave  $V_{saw}$  by a dual monostable multi-vibrator, an OR gate, a current regulative diode (CRD), and MOS FET. As shown in Fig. 10 (b), comparing the DC voltage  $V_{dvi}$ , which is generated by a resistance divider composed of  $R_1$  and  $R_2$ , and the sawtooth wave  $V_{saw}$ , the clock signal  $V_{CLK}$  is generated. Finally, inputting  $V_{sig}$  and  $V_{CLK}$  to D-Flipflop (D-FF),  $V_{g\_ATAC}$  is generated, which is input to its gate driver of the ATAC. The phase difference  $\pi/2 - \alpha$  between the output voltage of the

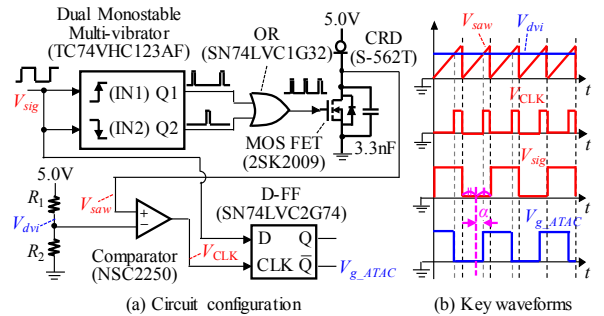


(a) Sensing circuit of transmitter current amplitude



(b) Generating circuit of gating signal for synchronous buck converter

Fig. 9. Controller of synchronous buck converter.



(a) Circuit configuration

(b) Key waveforms

Fig. 10. Phase shift circuit.

inverter and that of the ATAC is adjustable by the ratio of  $R_1$  and  $R_2$ . In the multiple-transmitter RIC-WPT system, the common signal  $V_{sig}$  is input to the gate driver of each inverter

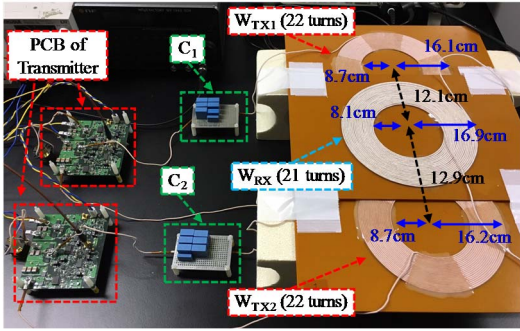


Fig. 11 Experimental setup.

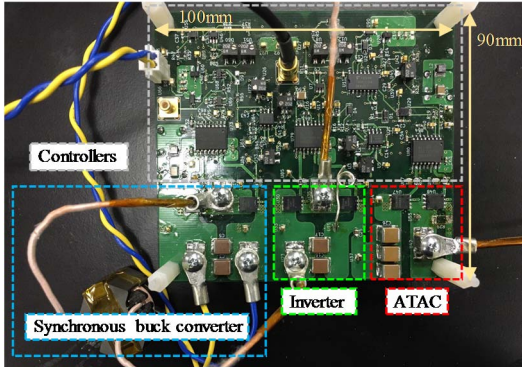


Fig. 12. PCB of each transmitter.

of the transmitter. Therefore, only designing  $\pi/2 - \alpha$ , the phase of the current in all transmitters is in phase and, as a result, all transmitters can fully compensate for the cross-interference effect.

#### IV. EXPERIMENTS

In this section, we carry out the experiment for the following three purposes. The first is to verify the load-independent transmitter current. The second is to verify the compensation of the cross-interference effect. The third is to test the influence of the ATAC on the overall efficiency of the RIC-WPT system.

##### A. Experimental Setup and Circuit Parameters

Fig. 11 shows the experimental setup for a multiple-transmitter RIC-WPT system.  $W_{RX}$  is placed vertically on  $W_{TX1}$  and  $W_{TX2}$  arrayed on the plane. The vertical distance between  $W_{RX}$  and each transmitter coil is 5.4 mm. The load of the receiver is comprised of the half-wave rectifier and an electrical load  $R_L$ . Fig. 12 shows the printed circuit board (PCB) of the transmitter including the synchronous buck converter, inverter, the ATAC, and these controllers. In this experiment, the gating signal of each inverter is common, which is the reference signal for the gating signal of each ATAC.

Table I shows circuit parameters. As shown in Table I,  $C_1$  and  $C_2$  differ depending on whether the ATAC is applied to the transmitter or not, respectively. Without the ATAC,  $C_1$  and  $C_2$  are designed so that each transmitter can operate the slightly inductive at the operating frequency to achieve ZVS turn-on and high power factor simultaneously. Specifically, the phase difference between the transmitter current and the output voltage of the inverter is  $14.4^\circ$ , which is designed based on the parasitic capacitors of MOS FETs, and transmitter currents. With the ATAC,  $C_1$  and  $C_2$  are designed based on (3) and (4) so that  $V_{A1}$  and  $V_{A2}$  can be positive. In this condition, the ATAC can achieve ZVS turn-on. Furthermore,  $C_r$  is

TABLE I CIRCUIT PARAMETERS FOR EXPERIMENTS

Symbols / Parameters		Values
$L_1$	Self-inductance of $W_{TX1}$	78.05 $\mu$ H
$L_2$	Self-inductance of $W_{TX2}$	78.39 $\mu$ H
$L_r$	Self-inductance of $W_{RX}$	73.59 $\mu$ H
$r_1$	Parasitic resistance of transmitter 1	0.16 $\Omega$
$r_2$	Parasitic resistance of transmitter 2	0.16 $\Omega$
$r_r$	Parasitic resistance of receiver	0.11 $\Omega$
$C_1$	Capacitance of transmitter 1 (without ATAC)	32.53 nF
$C_2$	Capacitance of transmitter 2 (without ATAC)	32.35 nF
$C_1$	Capacitance of transmitter 1 (with ATAC)	34.33 nF
$C_2$	Capacitance of transmitter 2 (with ATAC)	34.35 nF
$C_r$	Capacitance of receiver	33.16 nF
$C_A$	Smoothing capacitance of ATAC	10.0 $\mu$ F
$C_{det}$	Capacitance for detecting $I_1$ and $I_2$	6.8 $\mu$ F
$M_{12}$	Mutual inductance between $W_{TX1}$ and $W_{TX2}$	-0.71 $\mu$ H
$M_{1r}$	Mutual inductance between $W_{TX1}$ and $W_{RX}$	5.74 $\mu$ H
$M_{2r}$	Mutual inductance between $W_{TX2}$ and $W_{RX}$	5.60 $\mu$ H
$I_1, I_2$	Transmitter current	4.0 A
$f_{s,i}$	Operating frequency of inverter	100.0 kHz
$f_{s,b}$	Operating frequency of synchronous buck converter	170.0 kHz
$V_{dc}$	Input voltage of synchronous buck converter	20.0 V
$\alpha$	Designed phase difference	14.4 degrees

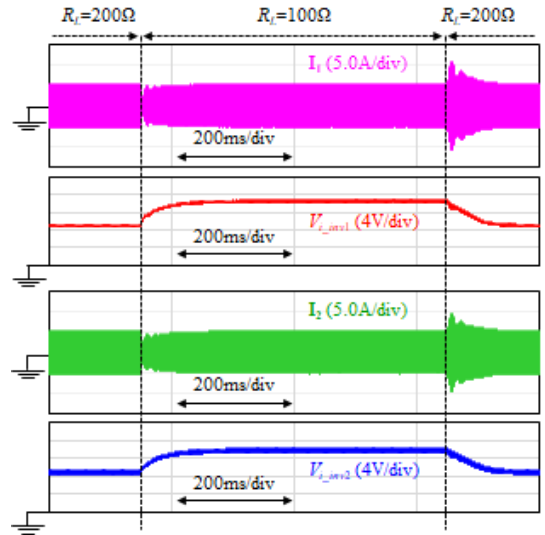


Fig. 13. Experimental results of load variation.

designed to resonate with  $L_r$  at the operating frequency of the inverter.

##### B. Load-Independent Transmitter Current

In this experiment, the load-independent transmitter current is evaluated under the load variation of the receiver. Fig. 13 shows the input voltage of the inverter and transmitter current waveforms during load variation in each transmitter. The load resistance  $R_L$  decreases to 100  $\Omega$  from 200  $\Omega$  and raise to 200  $\Omega$  from 100  $\Omega$  rapidly by an electrical load. As shown in Fig. 13, the amplitude of each transmitter current is constant in the steady-state even in load variation.

However, during this load variation, the worst transient speed is 120 ms, which is that of the load raising in transmitter 2. In addition to this, the maximum overshoot of the current is 114% in transmitter 1 when the load raises. Although the amplitude of each transmitter current is independent of the load in the steady-state, the improvement of the control performance in the aspect of the transient speed and overshoot is needed. The optimization of control parameters for improvement of the control performance will be studied in a future paper.

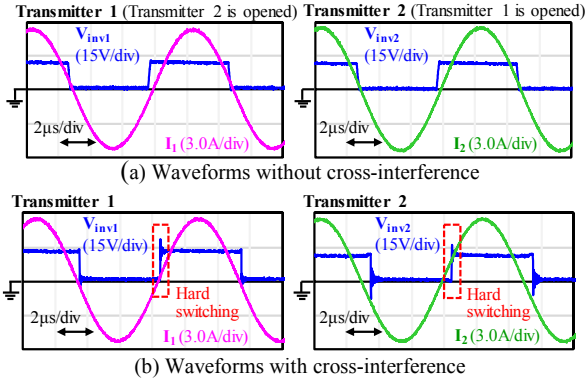


Fig. 14. Experimental waveforms without ATAC.

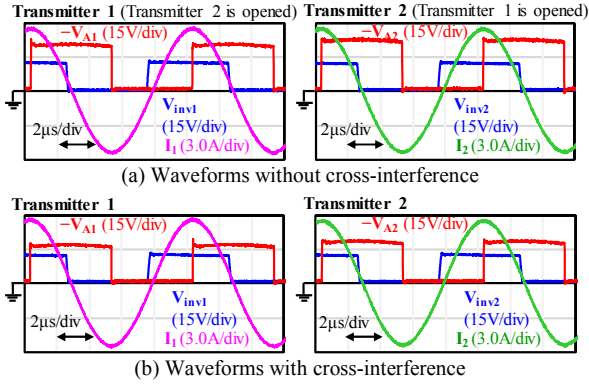


Fig. 15. Experimental waveforms with ATAC.

### C. Compensation for Cross-Interference

Next, we verify the proposed multiple-transmitter can compensate for the effect of the cross-interference comparing with the multiple-transmitter without ATAC. In this experiment, in order to clear that the compensation of the cross-interference effect can be achieved, the amplitude of the induced voltage on the transmitter due to the receiver is fixed in any case by adjusting the electrical load manually. In the above condition, Fig. 14 and Fig. 15 show the operating waveforms of each transmitter without ATAC and with ATAC, respectively.

Fig. 14 (a) shows the operating waveforms when each transmitter operates separately (an unmeasured side of the transmitter resonator is opened.). In this condition, each transmitter achieves ZVS turn-on and high power factor because there is no cross-interference. Fig. 14 (b) shows the operating waveforms when two transmitters operate simultaneously. As shown in Fig. 14 (b), the phase of the transmitter current advances against that of the output voltage of the inverter in each transmitter. These results indicate that each transmitter cannot achieve ZVS turn-on and operates under hard switching due to the cross-interference. In this experiment, the effective value of the current in each transmitter is 4 A and the operating frequency is 100 kHz. Hence, the cross-interference effect seems not to be a serious problem based on the experimental results. However, if the output power and operating frequency increase in the future, hard switching is a serious problem.

Fig. 15 (a) and Fig. 15 (b) show the waveforms of the proposed transmitter when a single transmitter operates or when two transmitters operate simultaneously, respectively. As shown in Fig. 15 (b), the phase of the transmitter current is fixed to be  $\pi/2$  against that of the output voltage of the ATAC. Then, the phase difference between the transmitter current and

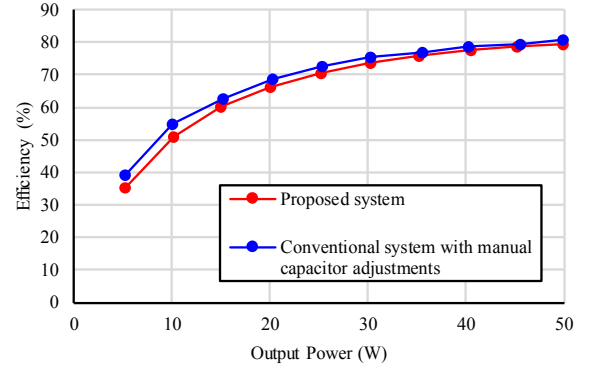


Fig. 16. Comparison of overall efficiencies in RIC-WPT system.

the output voltage of the inverter is kept, which achieves ZVS turn-on and high power factor, in each transmitter even if cross-interference occurs. Therefore, the proposed multiple-transmitter can compensate for the cross-interference.

### D. Overall Efficiency in RIC-WPT System

Finally, we evaluate whether the efficiency degradation due to the ATACs insertion can be a significant problem. In this subsection, we compare the dependence of the overall efficiency on the output power of the following two systems. The first system is the proposed multiple-transmitter RIC-WPT system (i.e., with ATACs). The second is the conventional multiple-transmitter RIC-WPT system (i.e., without ATACs).

In the conventional system, to eliminate the cross-interference effect, the resonant capacitors were tuned manually according to the output power based on (1) and (2). As a result, the phase difference  $\alpha$  of the conventional system can be fixed even if there is the cross-interference effect. On the other hand, in the proposed system, the capacitances of the resonant capacitors were fixed to the parameters in Table I. The output power was adjusted by changing the resistance of the electrical load. The other circuit parameters were the same as the values provided in Table I.

Fig. 16 shows the overall efficiency of each RIC-WPT system under various output power conditions. As shown in Fig. 16, each efficiency decreases as the output power decreases. The degradation of the efficiency may be mainly caused by the switching power loss of the synchronous buck converter because the switching loss becomes relatively high under low output power condition. However, the difference between each overall efficiency is slight under all output power conditions. Therefore, the ATAC can be considered not to be the main cause to decrease the efficiency and, accordingly, inserting the ATAC to the transmitter is not a significant problem in the aspect of the overall efficiency in the RIC-WPT system.

## V. CONCLUSION

Although the multiple-transmitter has many attractive features, the multiple-transmitter often suffers from power factor reduction and hard switching due to the cross-interference. Therefore, this paper proposed the multiple-transmitter and its controller that can eliminate the cross-interference effect automatically. In this paper, we found out that the cross-interference effect can be eliminated by controlling the reactance of each transmitter in order to keep the phase difference between the current and the output voltage in the transmitter. To achieve this control, the

proposed multiple-transmitter has the ATAC in each transmitter. The ATAC can maintain the phase difference between the current and the output voltage in the transmitter without any sensing of the transmitter currents as well as mutual inductances among transmitters, resulting in the elimination of the cross-interference effect. Besides, the proposed multiple-transmitter achieved the load-independent transmitter current by the control of the input voltage for the inverter by using the synchronous buck converter. The load-independent transmitter current contributes to the elimination of the cross-interference among receivers due to the change of the transmitter current. The experiments of the two-transmitter RIC-WPT system verified the effectiveness and appropriateness of the proposed multiple-transmitter. The experimental results showed that the proposed multiple-transmitter could achieve the load-independent transmitter current and the compensation of the cross-interference between the transmitters with almost no reduction in the efficiency. The results suggest that the proposed multiple-transmitter can be a key technology to realize a wide charging area RIC-WPT system.

#### REFERENCES

- [1] J. Zhou, B. Luo, X. Zhang, and Y. Hu, "Extendible load-isolation wireless charging platform for multi-receiver applications," *IET Power Electron.*, vol. 10, no. 1, pp. 134–142, Jan. 2017.
- [2] S. Seo, H. Jo, and F. Bien, "Free arrangement wireless power transfer system with a ferrite transmission medium and geometry-based performance improvement," *IEEE Trans. Power Electron.*, vol. 35, no. 5, pp. 4518–4532, May 2020.
- [3] M. Fu, T. Zhang, X. Zhu, P. C.-K. Luk, and C. Ma, "Compensation of cross coupling in multiple-receiver wireless power transfer systems," *IEEE Trans. Ind. Informat.*, vol. 12, no. 2, pp. 474–482, Apr. 2016.
- [4] J. Kuang, B. Luo, Y. Zhang, Y. Hu, and Y. Wu, "Load-isolation wireless power transfer with K-inverter for multiple-receiver applications," *IEEE Access*, vol. 6, pp. 31996–32004, 2018.
- [5] L. Jiang and D. Costinett, "A high-efficiency GaN-based single-stage 6.78 MHz transmitter for wireless power transfer applications," *IEEE Trans. Power Electron.*, vol. 34, no. 8, pp. 7677–7692, Aug. 2019.
- [6] M. Ishihara, K. Fujiki, K. Umetani, and E. Hiraki, "Automatic active compensation method of cross-coupling in multiple-receiver resonant inductive coupling wireless power transfer systems," in *Proc. IEEE Energy Convers. Congr. Expo.*, Baltimore, MD, USA, 2019, pp. 4584–4591.
- [7] Y. H. Sohn, B. H. Choi, E. S. Lee, G. C. Lim, G.-H. Cho, and C. T. Rim, "General unified analyses of two-capacitor inductive power transfer systems: equivalence of current-source SS and SP compensations," *IEEE Trans. Power Electron.*, vol. 30, no. 11, pp. 6030–6045, Nov. 2015.
- [8] S. Li, W. Li, J. Deng, T. D. Nguyen, and C. C. Mi, "A double-sided LCC compensation network and its tuning method for wireless power transfer," *IEEE Trans. Vehicular Technology*, vol. 64, no. 6, pp. 2261–2273, Jun. 2015.
- [9] W. Kim and D. Ahn, "Efficient deactivation of unused LCC inverter for multiple transmitter wireless power transfer," *IET Power Electron.*, vol. 12, no. 1, pp. 72–82, Jan. 2019.
- [10] Y. Li, R. Mai, L. Lu, T. Lin, Y. Liu, and Z. He, "Analysis and transmitter currents decomposition based control for multiple overlapped transmitters based WPT systems considering cross couplings," *IEEE Trans. Power Electron.*, vol. 33, no. 2, pp. 1829–1842, Feb. 2018.
- [11] S. Hui and D. Ahn, "Two-transmitter wireless power transfer with optimal activation and current selection of transmitters," *IEEE Trans. Power Electron.*, vol. 33, no. 6, pp. 4957–4967, June 2018.
- [12] D. Ahn and S. Hong, "Effect of coupling between multiple transmitters or multiple receivers on wireless power transfer," *IEEE Trans. Ind. Electron.*, vol. 60, no. 7, pp. 2602–2613, Jul. 2013.
- [13] Y. Endo, and Y. Furukawa, "Proposal for a new resonance adjustment method in magnetically coupled resonance type wireless power transmission," in *Proc. Int. Microw. Workshop Series on Innovative Wireless Power Transmission: Tech., Syst., and Appl.*, Kyoto, Japan, 2012, pp. 263–266.
- [14] C. Liu, A. P. Hu, B. Wang, and N.-K. C. Nair, "A capacitively coupled contactless matrix charging platform with soft switched transformer control," *IEEE Trans. Ind. Electron.*, vol. 60, no. 1, pp. 249–260, Jan. 2013.
- [15] Y. Lim, H. Tang, S. Lim, and J. Park, "An adaptive impedancematching network based on a novel capacitor matrix for wireless power transfer," *IEEE Trans. Ind. Electron.*, vol. 29, no. 8, pp. 4403–4413, Aug. 2014.
- [16] Z. Zhang, W. Ai, Z. Liang, and J. Wang, "Topology-reconfigurable capacitor matrix for encrypted dynamic wireless charging of electric vehicles," *IEEE Trans. Veh. Technol.*, vol. 67, no. 10, pp. 9284–9293, Oct. 2018.
- [17] J. Tian and A. P. Hu, "A DC-voltage-controlled variable capacitor for stabilizing the ZVS frequency of a resonant converter for wireless power transfer," *IEEE Trans. Power Electron.*, vol. 32, no. 3, pp. 2312–2318, Mar. 2017.
- [18] J. Osawa, T. Isobe, and H. Tadano, "Efficiency improvement of high frequency inverter for wireless power transfer system using a series reactive power compensator," in *Proc. IEEE Power Electron. Drive Syst. Conf. (PEDS2017)*, Honolulu, HI, USA, 2017, pp. 992–998.
- [19] A. Trigui, S. Hached, F. Mounaim, A. C. Ammari, and M. Sawan, "Inductive power transfer system with self-calibrated primary resonant frequency," *IEEE Trans. Power Electron.*, vol. 30, no. 11, pp. 6078–6087, Nov. 2015.
- [20] J.-U. W. Hsu, A. P. Hu, and A. Swain, "A wireless power pickup based on directional tuning control of magnetic amplifier," *IEEE Trans. Ind. Electron.*, vol. 56, no. 7, pp. 2771–2781, July 2009.
- [21] M. S. Perdigão, M. F. Menke, Á. R. Seidel, R. A. Pinto, J. M. Alonso, "A review on variable inductors and variable transformers: applications to lighting drivers," *IEEE Trans. Ind. Appl.*, vol. 52, no. 1, pp. 531–547, Jan.–Feb. 2016.